Plant Physiol. (1995) 107: 187–197

A Mutation in the D-*de* Loop of D_1 Modifies the Stability of the $S_2Q_A^-$ and $S_2Q_B^-$ States in Photosystem II[1]

Pirkko Mäenpää, Teresa Miranda, Esa Tyystjärvi, Taina Tyystjärvi, Govindjee, Jean-Marc Ducruet, Anne-Lise Etienne, and Diana Kirilovsky*

Department of Biology, University of Turku, SF-20500 Turku, Finland (P.M., E.T., T.T.); Section of Bioénergetique, Département de Biologie Cellulaire et Moléculaire, Institut National de la Recherche Agronomique/Comissariat de l'Energie Atomique-Saclay, 91190 Gif sur Yvette, France (T.M., J.-M.D.); Department of Plant Biology, University of Illinois, Urbana, Illinois 61801 (G.); and Photoregulation et Dynamique des Membranes Végétales, Unité de Recherche Associée 1810, Centre National de la Recherche Scientifique, Ecole Normale Superieure, 46 rue d'Ulm, 75230 Paris, France (A.-L.E., D.K.)

Photosystem II electron transfer, charge stabilization, and photoinhibition were studied in three site-specific mutants of the D_1 polypeptide of *Synechocystis* PCC 6803: E243K, E229D, and CA1 (deletion of three glutamates 242–244 and a substitution, glutamine-241 to histidine). The phenotypes of the E229D and E243K mutants were similar to that of the control strain (AR) in all of the studied aspects. The characteristics of CA1 were very different. Formate, which inhibits the Q_A^- to Q_B^- reaction, was severalfold less effective in CA1 than in AR. The $S_2Q_A^-$ and $S_2Q_B^-$ states were stabilized in CA1. It was previously shown that the electron transfer between Q_A^- and Q_B was modified in CA1 (P Mäenpää, T. Kallio, P. Mulo, G. Salih, E.-M. Aro, E. Tyystjärvi, C. Jansson [1993] Plant Mol Biol 22: 1–12). A change in the redox potential of the Q_A/Q_A^- couple, which renders the reoxidation of Q_A^- by back or forward reactions more difficult, could explain the phenotype of CA_1. Although the rates of photoinhibition measured as inhibition of oxygen evolution, Chl fluorescence quenching, and decrease of thermoluminescence B and Q bands were similar in AR and CA1, the CA1 strain more quickly reached a state from which the cells were unable to recover their activity. The results described in this paper suggest that a modification in the structure of the D-*de* loop of D_1 could influence the properties of the couple Q_A/Q_A^- in D_2 and the mechanism of recovery from photoinhibition.

The current model of the PSII core is based on the homology with the highly resolved structure of the photosynthetic reaction center of purple bacteria (Michel and Deisenhofer, 1988). PSII is formed by a heterodimer of the D_1 and D_2 polypeptides. It contains the chromophores and co-factors involved in charge separation and stabilization (Chl, pheophytin, quinones, etc.) (for reviews, see Babcock, 1987; Rutherford, 1989; Vermaas, 1991; Debus, 1992). Although a good homology exists between the L and D_1 polypeptides and M and D_2 polypeptides, D_1 and D_2 present additional extended sequences that are involved in the production of oxygen and possibly in the proteolysis of both proteins. The hydrophilic loops connecting the transmembrane helices D and E of D_1 and D_2, which are the binding sites of Q_B and Q_A, contain the extended sequences possibly related to the cleavage of the proteins in vivo. These regions in D_1 and D_2 are known as the D-*de* loop (amino acids 225–250 in D_1 and amino acids 224–248 in D_2). Q_A and Q_B are plastoquinones with different properties due to different protein environments. Q_A is usually singly reduced, whereas Q_B is a mobile two-electron acceptor. After primary charge separation, Q_A is reduced and then the electron is transferred to Q_B. This reaction is reversible, and in the dark there is an equilibrium between the states $Q_A^-Q_B$ and $Q_AQ_B^-$. After a second charge separation, Q_B becomes doubly reduced and protonated, and it leaves its site as Q_BH_2 by exchange with an oxidized plastoquinone (Velthuys, 1981; Wraight, 1981).

The Q_B pocket is also the binding domain of several classes of herbicides (Tischer and Strotmann, 1977; Trebst, 1986). By competing with Q_B, these molecules prevent the electron transfer between Q_A and Q_B and thus inhibit photosynthesis (Velthuys, 1981; Vermaas et al., 1983). It was shown that herbicide resistance results from mutations of one or two amino acids in the Q_B pocket region (for reviews, see Hirschberg et al., 1987; Vermaas, 1991). Since the presence of some of these herbicides in the Q_B pocket slows the proteolysis of D_1, it was proposed that the Q_B pocket was also the first site of light damage (Ohad et al., 1985). Moreover, a specific part of the hydrophilic loop between amino acids 238 and 249 was proposed to be the region of the first cleavage of D_1 in vivo (Greenberg et al., 1987).

[1] T.M. was supported by INIA (Spain). The Turku group was supported by the Foundation for Research of Natural Resources in Finland and the Academy of Finland. G. was supported by National Science Foundation grant 91–16838 (supplement 1994).

* Corresponding author; e-mail kirilov@biologie.ens.fr; fax 33–1–44–32–39–35.

Abbreviations: E_a, activation energy; F_i, fluorescence level attained in the absence of an inhibitor at the end of the fast photochemical increase; F_0, F_v, F_{max}, initial, variable and maximum Chl fluorescence; F_s, steady-state fluorescence level; Q_A and Q_B, primary and secondary plastoquinone electron acceptors of PSII; $t_{1/2}$, half-time.

The effect of modifications in the Q_B site on the electron transfer of PSII was analyzed in spontaneous herbicide-resistant mutants of *Chlamydomonas reinhardtii* (Erickson et al., 1989; Govindjee et al., 1992; Crofts et al., 1993) and in site-directed mutants of *Synechococcus* PCC 7942 (Ohad et al., 1990; Ohad and Hirschberg, 1990; Gleiter et al., 1992). We (Etienne et al., 1990; Kirilovsky et al., 1991; Perewoska et al., 1994) have especially studied the influence of mutations in the Q_B pocket on the electron transfer within PSII in herbicide-resistant mutants of *Synechocystis* 6714. The changes generally observed were, in most of the cases, due to a modification in the apparent equilibrium constant between $Q_A^-Q_B$ and $Q_AQ_B^-$ (Etienne et al., 1990). Two of these mutants also presented modifications on the donor side of the PSII probably induced by a long-range influence of the mutations in the Q_B pocket (Kirilovsky et al., 1991; Perewoska et al., 1994).

The influence of the Q_B pocket structure on the light sensitivity of PSII in these strains of *Synechocystis* was also studied (Kirilovsky et al., 1988, 1989, 1990; Perewoska et al., 1994). Exposure of photosynthetic organisms to high light intensity induces a quenching of fluorescence, an inhibition of the PSII activity, and a specific damage and proteolysis of D_1 (photoinhibition) (for a review, see Prasil et al., 1992). If exposure of photosynthetic cells to high light intensity is not too long, PSII activity can be restored. The well-known rapid turnover of D_1 is thought to allow functioning of PSII by counteracting photoinhibitory damage. We have demonstrated that two specific herbicide-resistant mutants of *Synechocystis* 6714, AzV ($Ala^{251}Val$, $Phe^{211}Ser$) and M_{35} ($Ala^{251}Val$), presented an increased high light sensitivity (Kirilovsky et al., 1988, 1989; Perewoska et al., 1994) in the sense that under light stress mutant cells more rapidly lost the ability to recover PSII activity than wild-type cells.

Most studies of the structure and function of the D-E hydrophilic loop were conducted in herbicide-resistant mutants or constructed mutants containing mutations in the sequence between amino acid 211 and amino acid 275, excluding the portion 220 to 247 (D-*de* loop). Very little is known about the structure and function of this segment of the loop.

In this paper we describe the influence of modifications in the extended sequence of the hydrophilic loop on the function of PSII. We utilized three site-specific mutants of *Synechocystis* 6803: E229D, E243K, and CA1 (Δ[E242-E244]; Q241H) (Mäenpää et al., 1993). The three site-specific mutants were constructed by the group in Turku, Finland, to test the role of the corresponding amino acids in the turnover of D_1. Two of the mutants, CA1 and E243K, have mutations in the QEEET motif in the Q_B pocket between amino acids 241 and 245, which was suggested to be the primary cleavage of D_1 in acceptor-side photoinhibition (Shipton et al., 1989). The third one, E229D, has a mutation in a PEST-like sequence, which may be a determinant for a rapid turnover of the protein (Rogers et al., 1986) and which is present just before the expected position of the D_1 cleavage. Tyystjärvi et al. (1994) have already demonstrated that, although the presence of the QEEET motif and the PEST-like sequence were not required for the cleavage of D_1, the rate of D_1 degradation was modified in these three mutants. Here we further characterize the influence of the three mutations on the electron transfer and charge stabilization in the PSII and the behavior of the cells under high light.

MATERIALS AND METHODS

Strains and Growth Conditions

As a control strain we used the strain AR of *Synechocystis* PCC 6803, which carries the same antibiotic resistance cassettes as the site-specific mutants but contains a wild-type *psb*A2 gene. The method of construction of the three mutants E229D, E243K, and CA1 is described elsewhere (Mäenpää et al., 1993). In the four strains, *psb*A2 is the only expressed copy of *psb*A coding for D_1. AR and mutant cells were grown in the mineral medium described by Herdman et al. (1973) with twice the concentration of nitrate, in the presence of antibiotics: 2.5 μg/mL streptomycin, 5 μg/mL spectinomycin, 5 μg/mL kanamycin, and 2.5 μg/mL chloramphenicol. The cells were grown in a rotatory shaker at 34°C in a CO_2-enriched atmosphere under illumination from fluorescent light of about 70 μE m^{-2} s^{-1}. The cells were then grown for several generations without antibiotics before each experiment.

Chl Determination

Chl content of *Synechocystis* cells was determined in methanol extracts according to the method of Bennet and Bogorad (1973).

Photoinhibition and Recovery Conditions

Cells were harvested by centrifugation and resuspended in fresh growth medium containing 50 mM Hepes (pH 6.8) at a final concentration of 30 μg Chl/mL. The cell suspension (35 mL) was incubated at 22°C in a glass tube (3 cm diameter) refrigerated by cooled water and illuminated by four Atralux spots of 150 W (each giving a photon flux density of about 1000 μE m^{-2} s^{-1}). The cells were gently stirred by a magnetic bar. At 30, 45, and 60 min, 10 mL of cell suspension was transferred from high light to low light. For the recovery, the cells were incubated at 34°C in a rotatory shaker under an illumination of 70 μE m^{-2} s^{-1}.

Photoinhibition was followed by fluorescence, thermoluminescence, and oxygen evolution measurements, and the recovery of the PSII activity was followed by fluorescence measurements.

Fluorescence Measurements and Determination of Herbicide Resistance and Formate Effect

Chl fluorescence induction during the first tens of milliseconds was monitored with a fluorimeter as described earlier (Vernotte et al., 1982). The fluorescence was excited with a tungsten lamp through CS 5–59 and CS 4–96 Corning (Corning, NY) filters. The fluorescence was detected in the red region through a CS 2–64 Corning filter and Wratten 90 filter. The recordings were made with a multichan-

nel analyzer. The cell suspension contained about 1 μg Chl/mL.

The inhibition of PSII electron transport from Q_A^- to Q_B resulting from the presence of increasing concentrations of herbicides was calculated by measuring the fluorescence level. The I_{50} shown in Table I is the concentration of the herbicide needed to obtain a value of 50 for the following ratio: $F_s - F_0/F_{max} - F_0$. F_0 is the initial fluorescence at the onset of illumination of the sample; F_{max} is the fluorescence level attained when a maximal concentration of Q_A^- is present; it was determined in the presence of a saturating concentration of DCMU (2×10^{-5} M); F_s is the intermediary fluorescence level when nonsaturating concentrations of herbicides lead to the closure of part of the centers.

We measured the inhibition of the electron transfer by different concentrations of formate by measuring the variable Chl fluorescence, i.e. fluorescence above the F_0 level, as described by Govindjee et al. (1990). The cells were diluted to 1 μg Chl/mL in a medium containing 20 mM Hepes (pH 6.5), 40 mM NaCl, and 5 mM $MgCl_2$. After different concentrations of formate were added, the cells were incubated in the dark for 10 min before the fluorescence measurements began.

Fluorescence relaxation in the presence of DCMU (10^{-5} M) was measured at 22°C with a pulse amplitude fluorimeter (PAM 101; Heinz Walz GmbH, Effeltrich, Germany) that was slightly modified to allow computer control of the measuring beam. A single turnover flash was generated with a xenon flash lamp (XST-103, Heinz Walz). The measuring beam of the fluorimeter was computer controlled to give bursts of 10-ms duration. The measurement consisted of five bursts of 1 Hz to measure the F_0 value, followed by one saturating flash and 30 bursts (each 10 ms long) of the measuring beam at defined intervals during 400 s. Finally, F_{max} was measured in continuous light. The short bursts of the measuring beam produced a stable F_0 level, and the 400-s period was long enough to let fluorescence relax back to the original F_0 level. The sample was at a concentration of 40 μg Chl/mL. To obtain the concentration of Q_A^- from the measurement of F_v the formula of Joliot et al. (1973) was applied to take into account the nonlinear relationship between Q_A^- and F_v. After this correction, with P = 0.45, the relaxation of Q_A^- was fitted with two exponentials. The control of the pulse amplitude fluorimeter and analysis of the data were done with the FIP fluorescence software (Q_A-Data, Turku, Finland).

Oxygen Measurements

Oxygen evolution of the cells of the four strains of *Synechocystis* 6803 (10 μg Chl/mL) was measured polarographically, with 2 mM 2,6-dichlorobenzoquinone in the growth medium, using a Clark-type oxygen electrode at 25°C. The samples were illuminated with saturating white light in the presence of two heat filters. Neutral density filters of 80, 50, 33, 10, and 1.8% of transmittance were used to obtain light saturation curves at different light intensities.

The amount of oxygen produced per flash during a sequence of saturating flashes was measured at 22°C with a rate electrode equivalent to that described by Joliot and Joliot (1968). The short (5 μs) saturating flashes were produced by a Strobotac (General Radio Co., Concord, MA). The spacing between flashes was 0.5 s. Cells were resuspended in a medium containing 20 mM Hepes (pH 6.5), 100 mM KCl, and 5 mM $MgCl_2$ at a concentration of about 150 μg Chl/mL, and they were dark adapted for 5 min at 22°C prior to each flash sequence (unless otherwise mentioned). The miss and double-hit parameters and the initial S_0 and S_1 apparent values were deduced using the "Sigma method" developed by Lavorel (1976). To measure the formate effect, formate was added to a final concentration of 40, 100, or 160 mM and preincubated in the dark for 10 min. The circulation medium contained the same concentration of formate.

Thermoluminescence Measurements

Thermoluminescence was measured in a home-built apparatus as described by Ducruet and Miranda (1992). In this set-up, which includes a cooled photomultiplier linked to a photon-counting system, dark-adapted samples can be rapidly cooled to −40°C after saturating flash(es) are fired at −10°C. During a slow, continuous warming (0.5°C/min) of the sample, luminescence is emitted when the temperature is sufficient to provide the activation energy needed for the recombination. The thermoluminescence B band is related to both $S_2Q_B^-$ and $S_3Q_B^-$ recombination, and the Q band obtained in the presence of DCMU is related to the $S_2Q_A^-$ reaction (Rutherford et al., 1982; Devault et al., 1983; Demeter and Vass, 1984). For measurements of the $S_2Q_B^-$ band, 20 preflashes were given to the samples and they were then incubated in the dark for 5 min at 22°C. For $S_2Q_A^-$ recombination studies, the sample was incubated with 5×10^{-5} M DCMU in the dark prior to the flash. A flash was given at −10°C and the sample was frozen rapidly in liquid nitrogen. The thermoluminescence signal observed upon heating the sample was analyzed as described earlier (Ducruet and Miranda, 1992). The thermoluminescence signal can be decomposed into elementary components determined by three parameters: E_a, the frequency factor (sk), and the number of charge pairs of which the recombination is detected. The multicomponent decomposition was started by a graphical simulation and followed by a numerical minimization (a procedure used to avoid false minima). Each component was computed step by step, using the experimental temperature scale (Ducruet and Miranda, 1992). The weighted sum of squares of the difference between the signal x_i and the simulation y_i, at sampling steps i, is minimized. The χ^2 statistic is defined as:

$$\chi^2 = \sum_{i=0}^{N} ((x_i - y_i)/\sigma_i)^2,$$

where N is the number of fitted data ($N > 100$) and σ_i is the error estimate for each particular point. The thermoluminescence data was obtained by photon counting. Since the random noise in photon counting is governed by Poisson's law, the standard deviation of the noise (σ) is the square root of the number of counts. The goodness of the fit is

given by the reduced $\chi^2 = \chi^2/N$, which should be 1 for a perfect fit.

RESULTS

Herbicide Sensitivity in CA1, E243K, and E229D Cells

The sensitivity of intact cells to herbicides was determined in AR and the site-specific mutant strains by monitoring the F_v in the presence of different concentrations of herbicides. Increasing concentrations of herbicides, which inhibit the electron transfer between Q_A^- and Q_B, produce an increase in the fluorescence level (F_s) related to the number of centers containing Q_A^-. The F_{max} is attained when the electron transfer between Q_A^- and Q_B is blocked by a saturating concentration of herbicide. Table I shows that the sensitivity to DCMU, atrazine, metribuzin, and ioxynil was similar in the site-specific mutants and in the control.

PSII Activity

Oxygen evolution in AR, E229D, E243K, and CA1 strains was measured at different light intensities. The maximum oxygen-evolving activity was about 550 μmol O_2 mg^{-1} Chl h^{-1} in the four strains. Moreover, the saturation curves were identical (data not shown). These results suggested that the strains have a similar number of active PSII centers and size of light-harvesting antenna.

Activation of dark-adapted samples by a train of saturating short flashes produces oxygen with a yield per flash that oscillates with a periodicity of four (Joliot et al., 1969; Kok et al., 1970). This is due to a cycle of five oxidation states (S-states: S_0–S_4) (Kok et al., 1970). In all of the strains studied in this report, the oscillations of oxygen produced per flash in dark-adapted samples displayed a maximum amount on the third flash and were similar (Fig. 1). As flashes proceed, the amplitude of the oscillations diminishes until a constant oxygen yield per flash is reached. This is due to double turnovers (double hits) occurring during the flash or to misses due to centers that have P^+ or Q_A^- before the flash or in which $P^+Q_A^-$ recombination occurs between the flashes (Shinkarev and Wraight, 1993). The miss and double-hit parameters and the initial S_0 and S_1 apparent values of the four strains (Table II) were similar.

Fluorescence measurements also give information about electron transfer in PSII. Three levels of fluorescence can be measured: F_0, F_{max}, and F_i. With *Synechocystis* in our experimental conditions, no thermal phase was observed, and during continuous illumination only the F_i level was reached. F_i corresponds to the concentration of Q_A^- stable under a given light intensity and is governed by three parameters: the apparent equilibrium between $Q_A^-Q_B$ and $Q_AQ_B^-$, the number of inactive centers, i.e. centers not connected to the plastoquinone pool, and the incident light intensity.

The F_0, F_{max}, and F_i levels were similar in the E243K, E229D, and AR strains (Table III). CA1 cells have higher F_{max} and F_i levels than AR cells. The ratio $(F_{max} - F_i)/F_0$ was similar in all of the strains.

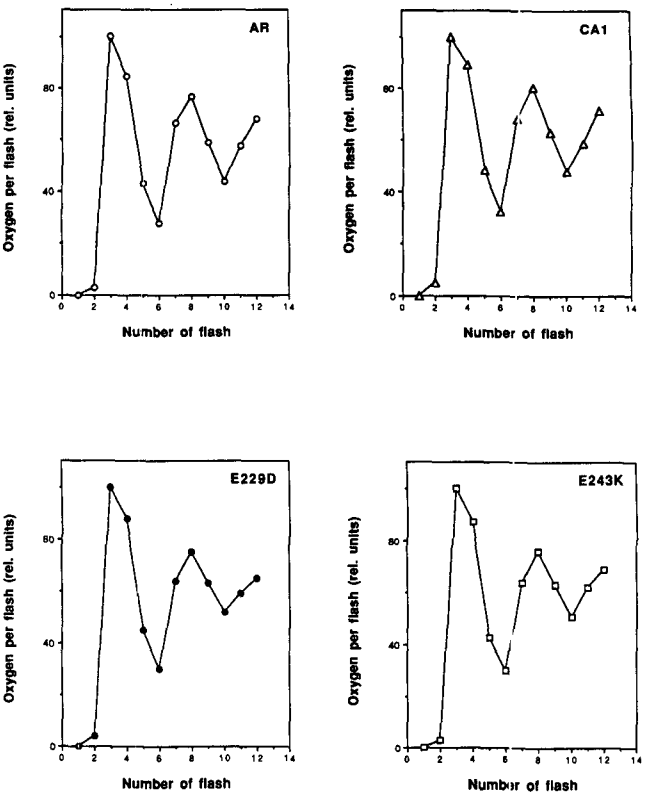

Figure 1. Oxygen yield (in relative units) per flash during a series of short saturating 0.5-s interval flashes in AR, E229D, E243K, and CA1 cells after 5 min of dark adaptation. The sequences shown are representative of each strain.

Table I. *I_{50} concentrations of different herbicides in the four strains of Synechocystis 6803 (AR, E229D, E243K, and CA1) determined from fluorescence measurements*

Strain	DCMU	Atrazine	Metribuzin	Ioxynil
	M	M	M	M
AR	1.8×10^{-7}	3×10^{-6}	1.8×10^{-6}	2.1×10^{-6}
E229D	2.3×10^{-7}	3.4×10^{-6}	2.3×10^{-6}	2.4×10^{-6}
E243K	1.8×10^{-7}	3×10^{-6}	1.8×10^{-6}	1.9×10^{-6}
CA1	1.8×10^{-7}	4.8×10^{-6}	1.8×10^{-6}	1.7×10^{-6}

Table II. *Oxygen sequence parameters*

The values of the oxygen sequence parameters were computed by the matrix analysis from recorded oxygen sequences on samples dark adapted for 5 min. S_0, S_1, Concentrations in the dark-adapted state; α, miss parameter; γ, double-hit parameter. The values vary in the limits given. This is due to various physiological parameters of the cells, which vary with the different batches.

Strain	% S_0	% S_1	α	γ
AR	37–42	58–63	0.11–0.145	0.03–0.05
E229D	37–43	57–63	0.12–0.145	0.03–0.05
E243K	38–42	58–62	0.12–0.15	0.03–0.05
CA1	38–44	56–62	0.10–0.135	0.03–0.05

Table III. *Fluorescence measurements*

Dark-adapted cells were illuminated with low light and the induction of fluorescence was enregistered. With the intensity of light used, we can see the increase of fluorescence to the F_{max} level, only in the presence of DCMU (10^{-5} M). The values of F_{max}, F_v, and F_i were normalized to F_0. The unnormalized F_0 level was similar in the four strains for the same light intensity and same Chl concentration.

Strain	F_0	F_{max}	$F_v(F_{max} - F_0)$	F_i	$(F_M - F_i)/F_0$
AR	1	2.45	1.45	0.3	1.37
E229D	1	2.5	1.5	0.4	1.40
E243K	1	2.47	1.47	0.4	1.37
CA1	1	2.73	1.73	0.52	1.42

Stability of the $S_2Q_B^-$ and $S_3Q_B^-$ States

We studied the stability of the $S_2Q_B^-$ and $S_3Q_B^-$ states by thermoluminescence measurements. The B bands of the E229D and E243K mutants were similar to those of the AR strain (data not shown). Figure 2 shows the thermoluminescence B band of AR and CA1 strains. The maximum of the B band produced after one saturating flash was at 35 to 38°C in AR and at 41 to 42°C in CA1 (Fig. 2). Both bands were dominated by one main peak. Sometimes, a small nonidentified component at about 45 to 48°C was present. A shoulder at 10 to 15°C, which corresponded to $S_2Q_A^-$ recombination, was also usually observed. From the B band, we calculated the E_a of the recombination reaction and the frequency number (sk) that give information about the probability that this reaction occurs (Table IV) (Devault et al., 1983; Devault and Govindjee, 1990). Both parameters influence the $t½$ of the $S_2Q_B^-$ state.

The back reaction $S_2Q_B^-$ was also studied with the oxygen rate electrode by varying the time between the first flash and the subsequent flashes (Bouges-Bocquet et al., 1973). The overall half-time of $S_2Q_B^-$ recombination determined by this method at 22°C was about 30 s for AR and 45 s for CA1. At 22°C the rate of $S_2Q_B^-$ recombination was 1.5 times slower in the CA1 mutant than in the AR strain.

The thermoluminescence band produced after two saturating flashes was not only related to the $S_2Q_B^-$ but also to the $S_3Q_B^-$ recombination. In AR, it could be simulated by two peaks with maxima at 35.3°C ($S_2Q_B^-$) and at 32.3°C ($S_3Q_B^-$) (Fig. 3; Table IV). We observed that the small component at 45 to 48°C present in AR after one flash also appeared after two flashes (Fig. 3). In CA1, the band could be simulated by two peaks with maxima at 41.5°C ($S_2Q_B^-$) and 40°C ($S_3Q_B^-$) (Fig. 3; Table IV). The B bands obtained after three and four flashes, which were also related to $S_2Q_B^-$ and $S_3Q_B^-$ recombinations, could be simulated with a combination of the two components of the signal observed after two flashes. The assignment of the peaks at 32°C in AR and 40°C in CA1 to the $S_3Q_B^-$ recombination was done by simulation of the B band after three flashes, where most of the luminescence come from this recombination reaction (data not shown).

The $t½$ of $S_3Q_B^-$ recombination reaction was determined with the oxygen rate electrode by varying the time between the second flash and the subsequent flashes. The $t½$ of the $S_3Q_B^-$ reaction was about 15 s for AR and 23 s for CA1 at 22°C.

The $S_2Q_A^-$ State

The main thermoluminescence band obtained after a flash in the presence of DCMU (the Q band) is related to the $S_2Q_A^-$ recombination (Rutherford et al., 1982; Demeter and Vass, 1984). A minor band at 40 to 50°C (C band), the precise origin of which remains uncertain, can also be observed under different conditions (for reviews, see Sane and Rutherford, 1986; Vass and Inoue, 1992). We will not discuss this minor band.

The AR, E229D, and E243K strains presented similar Q bands (data not shown). The thermoluminescence Q bands of AR and CA1 strains are shown in Figure 4. In the CA1 strain, the Q band, which was always broader than that in

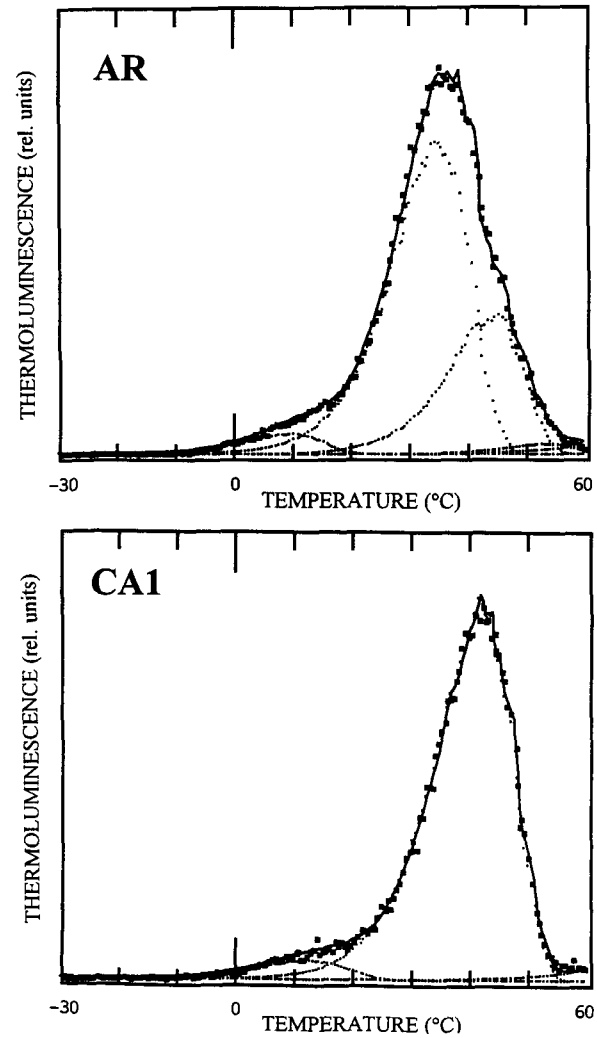

Figure 2. Thermoluminescence B band after one saturating flash (at −10°C) in AR and CA1. Shown are the measured thermoluminescence signal (■), the simulated components (– – –), and the sum of the different components (—). The parameters of the mean simulated peak of each B band are shown in Table IV. For fit procedure see "Materials and Methods." The fit was 1.52 for AR and 1.41 for CA1.

Table IV. *Thermoluminescence measurements: the B band*

Parameters of the main peaks of simulation of the thermoluminescence B bands obtained after one flash (related to $S_2Q_B^-$) and after two flashes (related to $S_2Q_B^-$ and to $S_3Q_B^-$) shown in Figures 2 and 3. The B bands obtained in five independent measurements could be simulated by the sum of components having about the same E_a (± 0.02) than the components described in this table. In all the cases the E_a corresponding to the B band of CA1 was higher than the one corresponding to the B band of AR. sk, Frequency number; temp., temperature of the maximum of each band.

Strain	State	E_a	sk	temp.
		eV		*°C*
AR (1F)	$S_2Q_B^-$	1.19	6.7×10^{15}	35.3
CA1 (1F)	$S_2Q_B^-$	1.22	7.15×10^{15}	42
AR (2F)	$S_3Q_B^-$	1.07	9.12×10^{13}	32.3
	$S_2Q_B^-$	1.19	6.7×10^{15}	35.3
CA1 (2F)	$S_3Q_B^-$	1.09	7.07×10^{13}	40
	$S_2Q_B^-$	1.22	7.3×10^{15}	41.5

the AR strain, was largely shifted toward higher temperatures. Two components were necessary to simulate correctly this band in both strains. The main peaks were at 4.5°C in AR and 13.4°C in CA1. The small ones were at 16.2 and 27.2°C in AR and CA1, respectively. The E_a and sk (frequency number) calculated from these simulations suggested that the $S_2Q_A^-$ state was also more stable in the CA1 strain (Table V).

There are several possible explanations for the combination of a large and a small component needed to fit the Q band. Luminescence depends on many factors (such as pH and electrochemical gradients, reaction center-antenna interaction), and local heterogeneities of these factors can lead to a widening of the thermoluminescence band emission, which could not be fitted by only one component. We can also suppose that the luminescence characteristics of PSII centers in formation or degradation processes are different from the mature PSII giving rise to the small component of the Q band. In other strains of cyanobacteria, such as *Synechocystis* 6803 and 6714, two components are also needed to fit the Q band (T. Miranda and D. Kirilovsky, unpublished data).

The thermoluminescence measurements were also done in the presence of different concentrations of DCMU to be sure that the component of the Q band at about 27°C in CA1 was not related to $S_2Q_B^-$ recombination. As an example, we show the thermoluminescence signal observed in the presence of 5×10^{-7} M DCMU (Fig. 5). The two components related to the Q band and the component related to the B band clearly appeared in the simulation of the signal.

The kinetics of the $S_2Q_A^-$ recombination reaction in the AR and CA1 strains were monitored by Chl fluorescence decay after a saturating flash in the presence of DCMU (Fig. 6). In this case, the decay of fluorescence corresponded to only the reoxidation of Q_A^- by positive charges stored on the donor side, the forward reaction being fully inhibited. The fluorescence yield decay could be fitted by two exponentials. The $t½$ of the faster component in the CA1 mutant was 2.2 and 1.4 s in AR and the half-times for the slower components were 88 s for CA1 and 63 s for AR. The kinetics of fluorescence decay, then, was slowed in the CA1 strain compared to the AR strain, confirming that the mutation in the CA1 mutant induced a stabilization of the $S_2Q_A^-$ state.

Formate Effect

Bicarbonate binds in the region of the Q_B pocket, and it can be displaced by formate, which inhibits the electron transfer between Q_A and Q_B. Bicarbonate can, in turn, act as a good competitor to formate, and when bicarbonate is added, the electron transfer is restored (for reviews, see

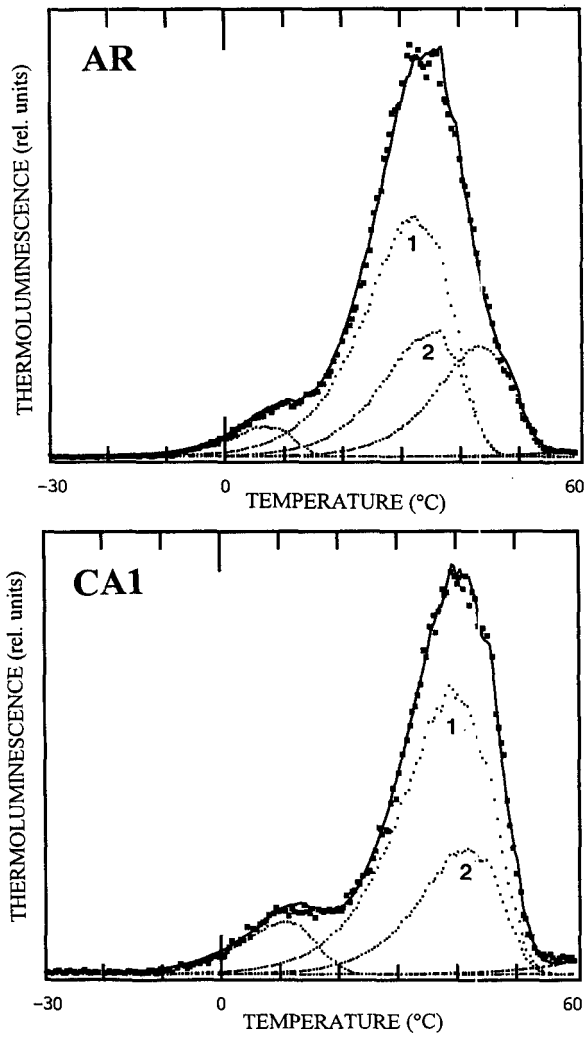

Figure 3. Thermoluminescence B band after two saturating flashes (at −10°C) in AR and CA1. Shown are the measured thermoluminescence signal (■), the simulated components (- - -), and the sum of the different components (—). Peak 1 is related to the $S_3Q_B^-$recombination, and peak 2 is related to the $S_2Q_B^-$ recombination. The parameters of components 1 and 2 are shown in Table IV. For fit procedure see "Materials and Methods." The fit is 3.3 for AR and 1.23 for CA1. We could not obtained a better fit for AR.

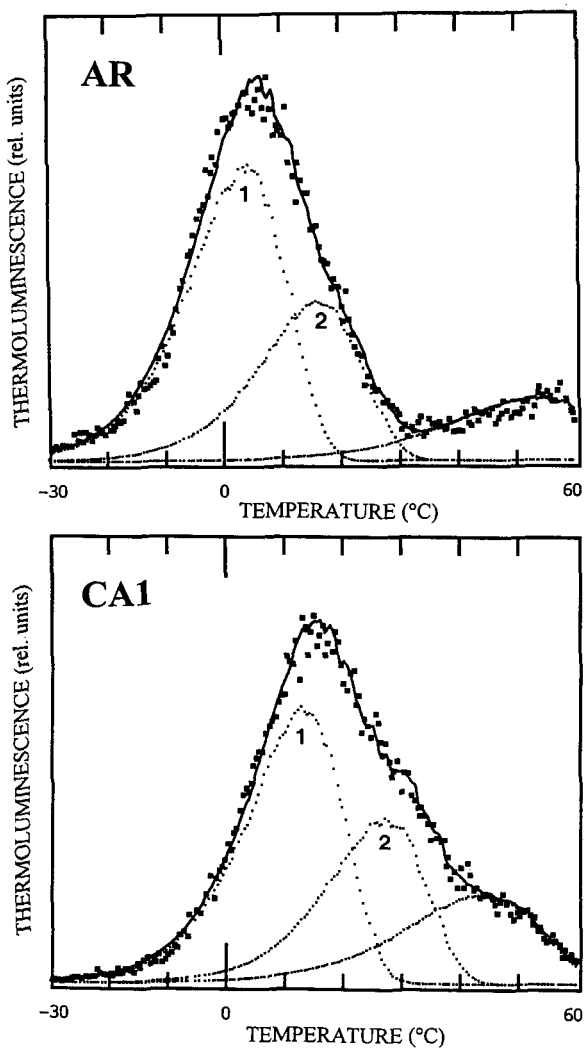

Figure 4. Thermoluminescence Q band after one saturating flash (at −10°C) in the presence of 5×10^{-5} M DCMU in AR and CA1. The measured thermoluminescence signal (■), the simulated components (– – –), and the sum of the different components (—) are shown. The fit is 1.74 for AR and 1.21 for CA1. The parameters of components 1 and 2 are described in Table V.

Blubaugh and Govindjee, 1988; Govindjee and van Rensen, 1993).

The sensitivity of PSII to formate-induced inhibition in the strains E229D, E243K, CA1, and the control AR was studied by fluorescence (Fig. 7A). AR, E229D, and E243K had the same sensitivity to formate; the maximum level of PSII inhibition (about 55%) was reached in the presence of 20 mM formate. In the CA1 mutant only 30% of the activity was inhibited and a much larger concentration of formate (160 mM) was needed to reach the maximum inhibitory level. Figure 7, B and C, shows the inhibition of oxygen evolution by formate in AR and CA1 strains. Forty millimolar formate inhibited about 40% of oxygen evolution in AR but no effect was observed in CA1 cells. One hundred sixty millimolar formate was needed to inhibit about 40% of the activity in this mutant.

Photoinhibition

We studied the behavior of AR and the site-specific mutant cells under high light illumination. During exposure of *Synechocystis* cells to high light, a specific quenching of F_{max} (with no quenching of F_0) was observed. It was followed by inhibition of the oxygen-evolving activity (Kirilovsky et al., 1988). In the experiments described in this paper, photoinhibition was done at 22°C to avoid recovery during the treatment (Kirilovsky et al., 1990). The photoinhibition was followed by fluorescence and flash-induced oxygen emission measurements. The kinetics of fluorescence quenching and of the inhibition of the oxygen emission were similar in the control and the three site-specific mutants (Fig. 8A).

We compared the rates of inhibition of Q_B^- and Q_A^- formation in CA1 and AR by following the decay of the thermoluminescence B band and Q band area during photoinhibition. The area of these bands is proportional to the quantity of centers where Q_B^- and Q_A^-, respectively, can be formed. The area of the B bands decreased slightly faster than that of the Q bands in both strains (Fig. 8B). The decay kinetics of the Q band and the B band in CA1 were similar to those in AR (Fig. 8B).

The PSII inhibition could be reversed if the cells were transferred to low light and growth temperature. The recovery of samples photoinhibited for 30, 45, and 60 min was followed by fluorescence measurements (Fig. 9). We observed that the duration of the photoinhibitory treatment influenced the rate of recovery in the four types of cells: the rate of F_v increase was smaller in the more stressed cells. Although the recovery rate was slightly slower in the E229D and E243K mutants than in AR, the cells of the three strains were still able to recover after 60 min of photoinhibition. In contrast, no recovery of F_v could be observed in CA1 cells exposed to high light for only 45 min (Fig. 9). Thus, this mutant reached sooner a state from which recovery was no longer possible.

DISCUSSION

We have described in this paper the characteristics of three site-specific mutants of *Synechocystis* 6803 with specific modifications in the hydrophilic loop of D_1 between the transmembrane D helix and the parallel *de* helix. Although this sequence of the protein is contiguous with the Q_B-binding niche, its role in the binding of Q_B or herbicides

Table V. *Thermoluminescence measurements: the Q band*

Parameters of the simulated bands (1 and 2) needed to fit the Q band of thermoluminescence signal obtained in the presence of DCMU in AR and CA1 shown in Figure 4. sk, Frequency number; temp., temperature of the maximum of each band.

Strain	Band	E_a	sk	temp.
		eV		°C
AR	1	0.75	8.74×10^9	4.5
	2	0.8	1.6×10^{10}	16.2
CA1	1	0.81	3.48×10^{10}	13.4
	2	0.88	1.08×10^{11}	27.2

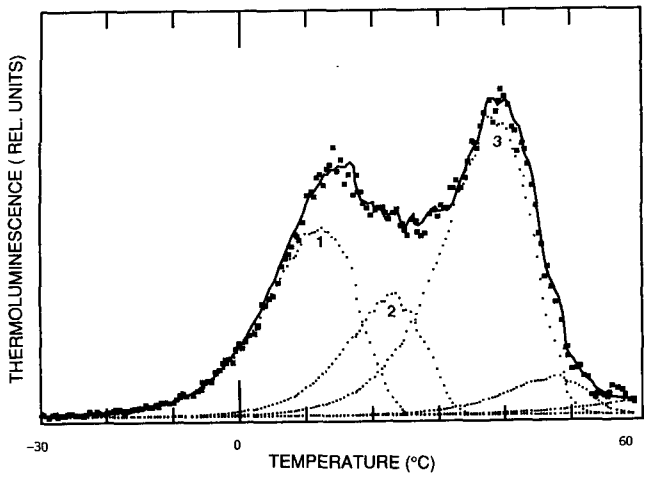

Figure 5. Thermoluminescence signal of CA1 after one saturating flash (at −10°C) in the presence of 5×10^{-7} M DCMU. The measured thermoluminescence signal (■), the simulated components (– – –), and the sum of the different components (—) are shown. Components 1 (Tm, 16.6°C) and 2 (Tm, 23.1°C) are related to the $S_2Q_A^-$ recombination (components of the Q band) and component 3 (Tm, 39°C) is related to the $S_2Q_B^-$ recombination (B band). The fit is 1.23.

or in the electron transfer between Q_A^- and Q_B is not known. We showed that herbicide sensitivity to four types of herbicide molecules (triazines, triazinones, methyl-urea, and phenolic herbicides) was not modified in the three mutants: E229D, E243K, and CA1 (Δ[E242-E244], Q241H) (Table I).

The electron transfer between Q_A^- and Q_B did not seem to be affected in the E229D and E243K mutants. The lifetimes and amplitudes of the three phases of the decay kinetics of the fluorescence yield after a saturating flash were similar in the E229D and E243K mutants and in the control (Mäenpää et al., 1993). No modification in the oxygen sequence (Table II; Fig. 1) and in the position of the thermoluminescence Q and B bands were observed (data not shown).

The CA1 mutant is very different from the other two mutants. Mäenpää et al. (1993) have already shown that the decay kinetics of the transient fluorescence yield after a saturating flash of CA1 were much slower than that of the AR strain. In CA1, the amplitude of the fast phase of fluorescence yield decay, which corresponds to the electron transfer from Q_A^- to Q_B or Q_B^-, was smaller and its lifetime was longer than in AR. The amplitude of the slow phase, which reflects the establishment of a quasi-steady-state level of Q_A^- and which is influenced by the binding and release of Q_B to and from its site, was larger and its lifetime was longer in CA1 than in AR (Mäenpää et al., 1993). Nevertheless, the level of fluorescence after 400 ms was similar in the control AR and in the CA1 mutant. A similar fluorescence phenotype was observed in one mutant of *C. reinhardtii*, DCMU-4 (S264A) (Etienne et al., 1990; Govindjee et al., 1992; Crofts et al., 1993). Crofts et al. (1993) demonstrated that the slow electron transfer in this mutant could be ascribed to a high dissociation constant for plastoquinone. Apart from the similarities in the fluorescence yield decay kinetics, the phenotype of CA1 is very different from that of the DCMU-4 mutant. In the present report, we describe other characteristics of the phenotype of CA1:

CA1 cells show a large resistance to formate, indicating that the binding of bicarbonate and/or the accessibility of formate and/or the competition between formate and bicarbonate probably were modified in this mutant.

Measurements of thermoluminescence and oxygen evolution showed that the back reactions, $S_2Q_B^-$ and $S_3Q_B^-$, were slower in CA1 than in AR, whereas in contrast, a destabilization of these states was generally observed in mutants presenting modifications of the Q_B pocket

The $S_2Q_A^-$ state was largely stabilized in the CA1 mutant as evidenced by a shift of the Q band of 10°C toward higher temperatures and by an increased half-time of the fluorescence and luminescence decay in the presence of DCMU. This stabilization seems larger than that of the $S_2Q_B^-$ and $S_3Q_B^-$ states.

Such an $S_2Q_A^-$ stabilization was never reported in other strains containing mutations in the D-E loop of D_1. However, a stabilization of this state was observed by two laboratories in a *Synechocystis* mutant lacking the 33-kD protein (Burnap et al., 1992; Vass et al., 1992). Both groups showed a decreased yield and a large damping (increased miss factor) of the flash pattern of oxygen evolution in the mutant because of alterations in the kinetics properties of the water-oxidizing complex. In contrast, in the CA1 mutant the oscillatory oxygen pattern was similar to that in the wild type (AR) and the misses were not increased, suggesting that the kinetics properties of the water-oxidizing complex was not modified in CA1.

The results presented in this report for the CA1 mutant can be explained by a modification of the redox couple Q_A/Q_A^-, which may render the reoxidation of Q_A^- by forward or back reactions more difficult. The fact that a change in the structure of the D-*de* loop of D_1 induced a modification of the properties of the couple Q_A/Q_A^- sug-

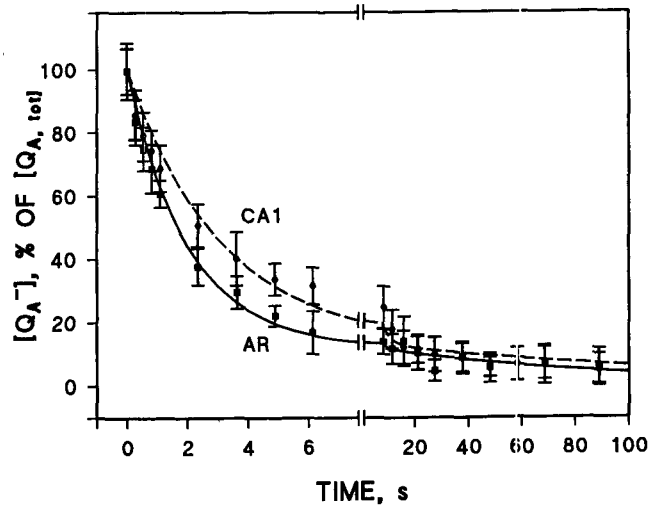

Figure 6. Fluorescence yield decay after a saturating flash in dark-adapted cells of AR (■) and CA1 (●) strains in the presence of 10^{-5} M DCMU. The curves are averages of 12 measurements.

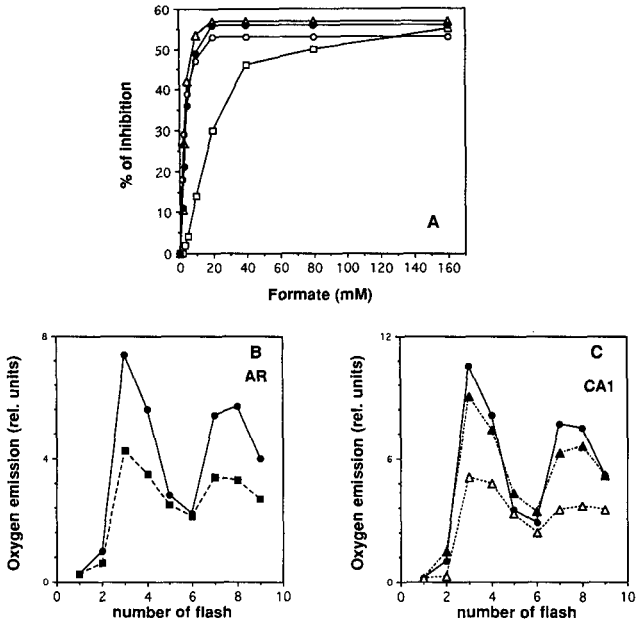

Figure 7. Formate effect. A, Inhibition of PSII activity as a function of formate concentration in cells of AR (●), E229D (△), E243K (○), and CA1 (□) strains. The inhibition of the PSII activity was followed by Chl fluorescence measurements. % Inhibition = *([Fmax − Fs]/[$F_{s_{formate}}$ − Fs]) × 100.* F_{max}, Fluorescence level in the presence of 10^{-5} M DCMU; F_s, steady-state fluorescence level without any addition; $F_{s_{formate}}$, steady-state fluorescence level in the presence of different concentrations of formate. In the presence of 10^{-5} M DCMU there was 100% inhibition of PSII activity. B and C, Oxygen yield per flash during a series of short saturating flashes spaced 0.5 s apart in the absence (●) or in the presence of 40 mM (■), 100 mM (▲), or 160 mM (△) formate in AR (B) and CA1 cells (C). For the formate treatment, see "Materials and Methods."

gests that this sequence of the D_1 protein is oriented toward the Q_A-binding site in D_2. Moreover, we observed that the E_a of the $S_2Q_A^-$ recombination reaction depended on the occupancy of the Q_B site by DCMU (data not shown). Trebst (1991) demonstrated that the presence of certain herbicides on the Q_B site slowed the trypsinization of D_2 and proposed that there was a direct interaction between the amino acids close to the Arg^{238} and Arg^{234} of the Q_B and Q_A sites, respectively.

On the other hand, Kless et al. (1993) have shown that structural modifications of the D-*de* loop of D_2 could change the properties of the redox couple Q_B/Q_B^-. They observed a large shift of the B band toward higher temperatures in several mutants containing a modified D-*de* loop in D_2. We conclude that most probably the mutation in the CA1 mutant (deletion of the glutamates 242 to 244 and change of Gln^{241} to His) caused only modifications in the structure of both quinone-binding sites. There is no need to invoke an additional modification on the donor side to explain our results.

In addition to the mutations described here, only one other mutation in the D-*de* loop has been reported: E242N (Ohad and Hirschberg, 1992). This mutant of *Synechocystis* 6803 did not present any change in the electron transfer between Q_A^- and Q_B or of the herbicide sensitivity. This result and the results of the present work suggest that point mutations in the portion of the D-E loop between the amino acids 220 and 247 do not modify the Q_B binding. Only a larger mutation, such as in CA1, which may cause a large change in the conformation of the loop, modifies the properties of both the Q_B pocket and adjacent Q_A pocket. Kless et al. (1993) mentioned the existence of mutants of this portion of D_1 that slightly influence Q_B binding. Unfortunately, no precise results have been published about these mutants. The Turku group is constructing new mutations in this portion of D_1 to study further the influence of this region of the protein on the electron transfer.

Regarding photoinhibition, we showed that the rates of decrease of the F_v, the oxygen-evolving activity, and the area of the Q band were similar in the four strains when the exposure to high light was made at 22°C. At this temperature, D_1 degradation, synthesis, and reassembly of PSII were slow enough not to counterbalance D_1 damage. The same rate of PSII inactivation in the four strains was also

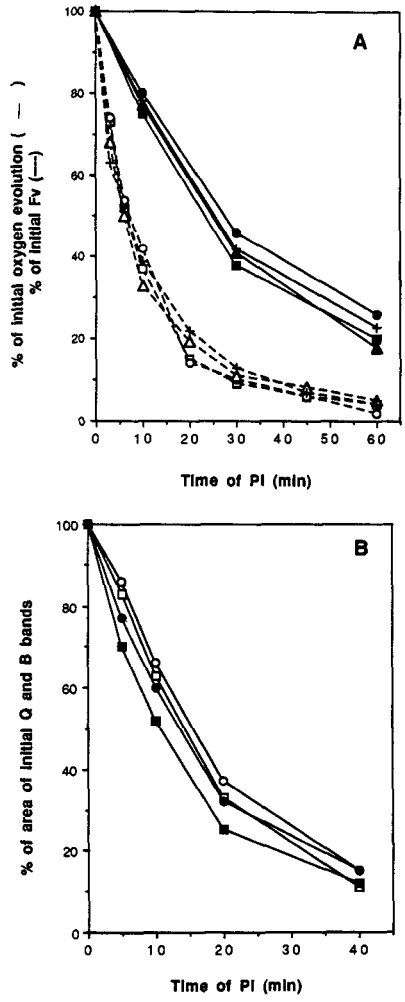

Figure 8. A, Decrease of F_v ($F_v = F_{max} - F_0$) (– – –) and inhibition of oxygen emission during photoinhibition (—) in AR (●), CA1 (■), E229D (▲), and E243K (+) cells. F_v/F_0 = 1.5 to 2 in nonphotoinhibited cells. F_0 did not vary during photoinhibition. B, Decrease of the areas of B (solid symbols) and Q (open symbols) bands in AR (●) and CA1 (■) cells during exposure to high light at 22°C.

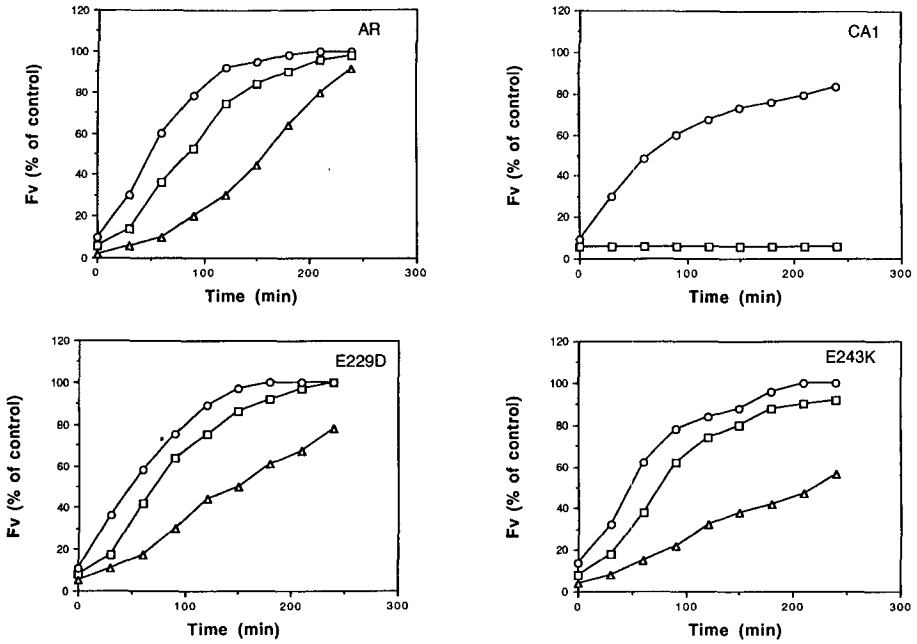

Figure 9. Recovery of F_v in AR, CA1, E229D, and E243K cells photoinhibited for 30 min (○), 45 min (□), and 60 min (△). F_0 was constant during the time of recovery.

observed when photoinhibition experiments were done in the presence of lincomycin (a protein synthesis inhibitor) (Tyystjärvi et al., 1994). These results are not sufficient to explain why the CA1 mutant reached faster a state from which the recovery from photoinhibition was no longer possible. A possible explanation for the phenotype of CA1 after prolonged photoinhibition is that a more severe disassembly of the PSII complex occurs in CA1 than in the control, involving degradation of other proteins in addition to D_1. We are currently testing this hypothesis.

Received August 1, 1994; accepted October 17, 1994.

LITERATURE CITED

Babcock GT (1987) The photosynthetic oxygen-evolving process. *In* J Amesz, ed, Photosynthesis. Elsevier, Amsterdam, The Netherlands, pp 125–158

Bennet A, Bogorad L (1973) Complementary chromatic adaptation in a filamentous blue-green alga. J Cell Biol **58:** 419–435

Blubaugh DJ, Govindjee (1988) The molecular mechanism of the bicarbonate effect at the plastoquinone reductase of photosynthesis. Photosynth Res **19:** 85–128

Bouges-Bocquet B, Benoun P, Taboury J (1973) Deactivation of oxygen precursors in presence of 3-(3,4-dichlorophenyl)-1,1,dimethylurea and phenylurethane. Biochim Biophys Acta **325:** 247–254

Burnap R, Shen J-R, Jursinic P, Inoue Y, Sherman L (1992) Oxygen yield and thermoluminescence characteristics of a cyanobacterium lacking the manganese-stabilizing protein of photosystem II. Biochemistry **31:** 7404–7410

Crofts A, Baroli I, Kramer D, Taoka S (1993) Kinetics of electron transfer between Q_A and Q_B in wild-type and herbicide-resistance mutants of *Chlamydomonas reinhardtii*. Z Naturforsch **48c:** 259–266

Debus RJ (1992) The manganese and calcium ions of photosynthetic oxygen evolution. Biochim Biophys Acta **1102:** 269–352

Demeter S, Vass I (1984) Charge accumulation and recombination in photosystem II studied by thermoluminescence. Biochim Biophys Acta **764:** 24–32

DeVault D, Govindjee (1990) Photosynthetic glow peaks and their relationship with the free energy changes. Photosynth Res **24:** 175–181

DeVault D, Govindjee, Arnold W (1983) Energetics of photosynthetic glow peaks. Proc Natl Acad Sci USA **80:** 983–987

Ducruet JM, Miranda T (1992) Graphical and numerical analysis of thermoluminescence and fluorescence F_0 emission in photosynthetic material. Photosynth Res **33:** 15–27

Erickson IM, Pfister K, Rahire M, Togasaki RK, Mets L, Rochaix JD (1989) Molecular and biophysical analysis of herbicide-resistant mutants of *Chlamydomonas reinhardtii*: structure-function relationship of the photosystem II D_1 polypeptide. Plant Cell **1:** 361–371

Etienne AL, Ducruet JM, Ajlani G, Vernotte C (1990) Comparative studies on electron transfer in photosystem II of herbicide-resistant mutants from different organisms. Biochim Biophys Acta **1015:** 435–440

Gleiter HM, Ohad N, Koike H, Hirschberg J, Renger G, Inoue Y (1992) Thermoluminescence and flash induced oxygen yield in resistant mutants of the D_1 protein in *Synechocystis* PCC 7942. Biochim Biophys Acta **1140:** 135–143

Govindjee, Eggenberg P, Pfister K, Strasser R (1992) Chlorophyll a fluorescence decay in herbicide resistant D_1 mutants of *Chlamydomonas reinhardtii* and the formate effect. Biochim Biophys Acta **1101:** 353–358

Govindjee, Van Rensen JJ S (1993) Photosystem II reaction center and bicarbonate. *In* J Deisenhofer, J Norris, eds, The Photosynthetic Reaction Center, Vol 1. Academic Press, New York, pp 357–389

Govindjee, Vernotte C, Peteri B, Astier C, Etienne A-L (1990) Differential sensitivity of bicarbonate-reversible formate effects on herbicide-resistant mutants of *Synechocystis* 6714. FEBS Lett **267:** 273–276

Greenberg BM, Gaber V, Mattoo AK, Edelman M (1987) Identification of a primary *in vivo* degradation product of the rapidly turning over 32 Kd protein of photosystem II. EMBO J **6:** 2865–2869

Herdman M, Deloney SF, Carr NG (1973) A new medium for the isolation and growth of auxotrophic mutants of the blue green alga *Anacystis nidulans*. J Gen Microbiol **79:** 233–237

Hirschberg J, Ben Yehuda A, Pecker I, Ohad N (1987) Mutations resistant to photosystem II herbicides. *In* D von Wettstein, N-H Chua, eds, Plant Molecular Biology. Plenum Press, New York, pp 357–366

Joliot P, Barbieri G, Chabaud R (1969) Un nouveau modèle des centres photochimiques du Système II. Photochem Photobiol **10:** 309–329

Joliot P, Bennoun P, Joliot A (1973) New evidence supporting energy transfer between photosynthetic units. Biochim Biophys Acta **305:** 317–328

Joliot P, Joliot A (1968) A polarographic method for detection of oxygen production and reduction of Hill reagent by isolated chloroplasts. Biochim Biophys Acta **153:** 625–634

Kirilovsky D, Ajlani G, Picaud M, Etienne AL (1989) Mutations responsible for high light sensitivity in an atrazine-resistant mutant of *Synechocystis* 6714. Plant Mol Biol **13:** 355–363

Kirilovsky D, Ducruet JM, Etienne AL (1990) Primary events occurring in photoinhibition in *Synechocystis* 6714 wild-type and an atrazine-resistant mutant. Biochim Biophys Acta **1020:** 87–93

Kirilovsky D, Ducruet JM, Etienne AL (1991) Apparent destabilization of the S_1 state related to herbicide resistance in a cyanobacterium mutant. Biochim Biophys Acta **1060:** 37–44

Kirilovsky D, Vernotte C, Astier C, Etienne AL (1988) Reversible and irreversible photoinhibition in herbicide-resistant mutants of *Synechocystis* 6714. Biochim Biophys Acta **933:** 124–131

Kless H, Oren-Shamir M, Ohad I, Edelman M, Vermaas W (1993) Protein modifications in the D2 protein of photosystem II affect properties of the Q_B/herbicide-binding environment. Z Naturforsch **48c:** 185–190

Kok B, Forbush B, McGloin M (1970) Cooperation of charges in photosynthetic O_2 evolution. I. A linear four steps mechanism of the reaction in chloroplast. Photochem Photobiol **11:** 457–475

Lavorel J (1976) Matrix analysis of the oxygen evolving system of photosynthesis. J Theor Biol **57:** 171–185

Mäenpää P, Kallio T, Mulo P, Salih G, Aro E-M, Tyystjärvi E, Jansson C (1993) Site-specific mutations in the D1 polypeptide affect the susceptibility of *Synechocystis* 6803 cells to photoinhibition. Plant Mol Biol **22:** 1–12

Michel H, Deisenhofer J (1988) Relevance of the photosynthetic reaction center from purple bacteria to the structure of photosystem II. J Biochem **27:** 1–7

Ohad I, Kyle DJ, Arntzen CJ (1985) Membrane protein damage and repair removal and replacement of inactivated 32 Kd polypeptide in chloroplast membranes. J Cell Biol **99:** 481–485

Ohad N, Amir-Shapira D, Koike H, Inoue Y, Ohad I, Hirschberg J (1990) Amino-acids substitutions in the D_1 protein of photosystem II affect Q_B^- stabilization and accelerate turnover of D_1. Z Naturforsch **45c:** 402–408

Ohad N, Hirschberg J (1990) A similar structure of the herbicide binding site in photosystem II of plants and cyanobacteria is demonstrated by site specific mutagenesis of the *psb*A gene. Photosynth Res **23:** 73–79

Ohad N, Hirschberg J (1992) Mutations in the D_1 subunit of photosystem II distinguish between quinone and herbicide binding sites. Plant Cell **4:** 273–282

Perewoska I, Etienne A-L, Miranda T, Kirilovsky D (1994) S_1 destabilization and higher sensitivity to light in metribuzin-resistant mutants. Plant Physiol **104:** 235–245

Prasil O, Adir N, Ohad I (1992) Dynamics of photosystem II: mechanism of photoinhibition and recovery processes. *In* J Barber, ed, The Photosystems: Structure, Function and Molecular Biology. Elsevier Science Publishers BV, Amsterdam, The Netherlands, pp 295–348

Rogers S, Wells R, Rechsteiner M (1986) Amino acid sequences common to rapidly degraded proteins: the PEST hypothesis. Science **234:** 3990–3998

Rutherford AW (1989) Photosystem II, the water-splitting enzymol. Trends Biochem Sci **14:** 227–232

Rutherford AW, Crofts AR, Inoue Y (1982) Thermoluminescence as a probe of photosystem II photochemistry. The origin of the flash-induced glow peaks. Biochim Biophys Acta **682:** 457–465

Sane PV, Rutherford AW (1986) Thermoluminescence from photosynthetic membranes. *In* Govindjee, J Amesz, DC Fork, ed, Light Emission by Plants and Bacteria. Academic Press, New York, pp 329–361

Shinkarev V, Wraight C (1993) Oxygen evolution in photosynthesis: from unicycle to bicycle. Proc Natl Acad Sci USA **90:** 1834–1838

Shipton CA, Marder JB, Barber J (1989) Determination of catabolism of the photosystem II D1 subunit by structural motifs in the polypeptide sequence. Z Naturforsch **45c:** 388–394

Tischer W, Strotmann H (1977) Relationship between inhibitor binding of chloroplasts and inhibition of photosynthetic electron transport. Biochim Biophys Acta **460:** 113–125

Trebst A (1986) The topology of plastoquinone and herbicide binding peptides of photosystem II in the thylakoid membrane. Z Naturforsch **41c:** 240–245

Trebst A (1991) A contact site between the two reaction center polypeptides of photosystem II is involved in photoinhibition. Z Naturforsch **46c:** 557–562

Tyystjärvi T, Aro E-M, Jansson C, Mäenpää P (1994) Changes of amino acid sequence in PEST-like area and QEEET motif affect degradation rate of D1 polypeptide in photosystem II. Plant Mol Biol **25:** 517–526

Vass I, Cook K, Deak Z, Mayes S, Barber J (1992) Thermoluminescence and flash-oxygen characterization of the IC2 deletion mutant of *Synechocystis* sp. PCC 6803 lacking the photosystem II 33 kDa protein. Biochim Biophys Acta **1102:** 195–201

Vass I, Inoue Y (1992) Thermoluminescence in the study of photosystem II. *In* J Barber, ed, Topics in Photosynthesis, Vol II: The Photosystems: Structure, Function and Molecular Biology. Elsevier, Amsterdam, The Netherlands, pp 259–294

Velthuys B (1981) Electron-dependent competition between plastoquinone and inhibitors for binding to photosystem II. FEBS Lett **126:** 277–281

Vermaas WJF (1991) Photosystem II. *In* L Bogorad, IK Vasil, eds, The Photosynthetic Apparatus: Molecular Biology and Operation. Academic Press, New York, pp 3–25

Vermaas WFJ, Renger G, Arntzen CJ (1983) Herbicide/quinone binding interactions in photosystem II. Z Naturforsch **39c:** 368–373

Vernotte C, Etienne AL, Briantais JM (1982) Analysis of the kinetics of the cation-induced increase in photosystem II fluorescence in isolated thylakoids. Biochim Biophys Acta **545:** 519–527

Wraight CA (1981) Oxidation-reduction physical chemistry of the acceptor quinone complex in bacterial photosynthetic reaction centers: evidence for a new model of herbicide activity. Isr J Chem **21:** 348–354